MODELLING SUPERNOVAE IN THEIR NEBULAR PHASE

Anders Jerkstrand

Stockholm University
European Research Council
Swedish Research Council

History of late-time SN observations

- From ~ 100 – 1000d post explosion.
- Powering by ^{56}Ni→^{56}Co→^{56}Fe.

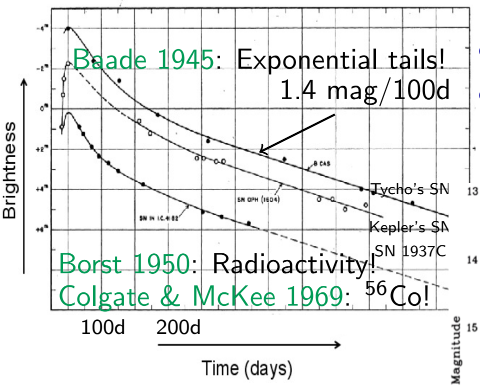

Baade 1945: Exponential tails! 1.4 mag/100d

Borst 1950: Radioactivity!

Colgate & McKee 1969: ^{56}Co!

Filippenko+1986: First good-quality nebular spectrum of a SN.

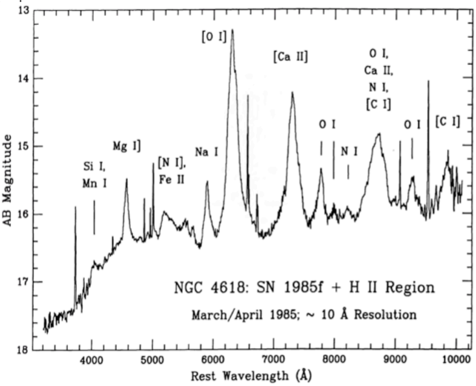

Late-time spectral modelling : 40 years of progress

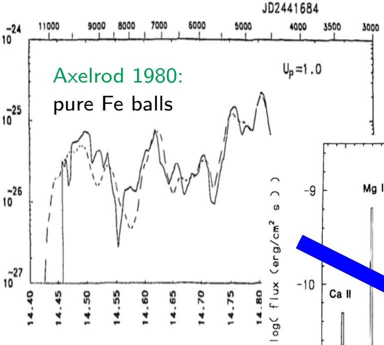

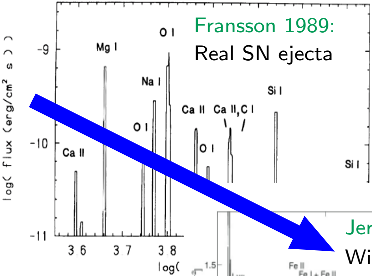

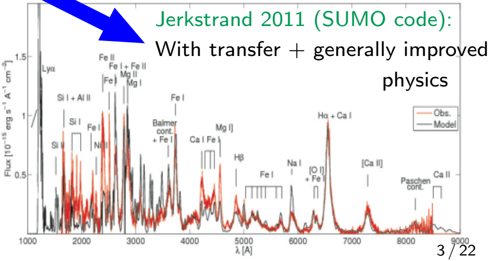

- Radioactive deposition
  - Non-thermal electrons
    - NLTE ionization and excitation
      - Temperature
        - Atomic data
          - Mixing treatment
            - Radiate transfer
              - Molecules and dust

Nebular phase analysis - pros and cons

Photospheric phase → Nebular phase → Remnant phase

Pros:

- Probes the core of the exploded star - SN nucleosynthesis can be inferred.

Nebular phase analysis - pros and cons

Photospheric phase → Nebular phase → Remnant phase

Pros:

- Probes the core of the exploded star - SN nucleosynthesis can be inferred.
- Line profiles diagnose the 3D structure and link to explosion physics.

Nebular phase analysis - pros and cons

Photospheric phase → Nebular phase → Remnant phase

Pros:

- Probes the core of the exploded star - SN nucleosynthesis can be inferred.
- Line profiles diagnose the 3D structure and link to explosion physics.
- Less line blending than photospheric phase (lower v and T for emitting gas).

Nebular phase analysis - pros and cons

Photospheric phase → Nebular phase → Remnant phase

Pros:

- Probes the core of the exploded star - SN nucleosynthesis can be inferred.
- Line profiles diagnose the 3D structure and link to explosion physics.
- Less line blending than photospheric phase (lower v and T for emitting gas).
- Limited radiative transfer effects → relatively "clean view".

Nebular phase analysis - pros and cons

Photospheric phase → Nebular phase → Remnant phase

Pros:

- Probes the core of the exploded star - SN nucleosynthesis can be inferred.
- Line profiles diagnose the 3D structure and link to explosion physics.
- Less line blending than photospheric phase (lower v and T for emitting gas).
- Limited radiative transfer effects → relatively "clean view".

Cons:

- Complex (mostly NLTE) modelling, and associated challenge in getting physical conditions right.

Nebular phase analysis - pros and cons

Photospheric phase → Nebular phase → Remnant phase

Pros:

- Probes the core of the exploded star - SN nucleosynthesis can be inferred.
- Line profiles diagnose the 3D structure and link to explosion physics.
- Less line blending than photospheric phase (lower v and T for emitting gas).
- Limited radiative transfer effects → relatively "clean view".

Cons:

- Complex (mostly NLTE) modelling, and associated challenge in getting physical conditions right.
- Complex mixing in the explosion (macroscopic, maybe some microscopic). Most modelling so far limited to 1D with artificial mixing and can only partly account for this.

Nebular phase analysis - pros and cons

Photospheric phase → Nebular phase → Remnant phase

Pros:

- Probes the core of the exploded star - SN nucleosynthesis can be inferred.
- Line profiles diagnose the 3D structure and link to explosion physics.
- Less line blending than photospheric phase (lower v and T for emitting gas).
- Limited radiative transfer effects → relatively "clean view".

Cons:

- Complex (mostly NLTE) modelling, and associated challenge in getting physical conditions right.
- Complex mixing in the explosion (macroscopic, maybe some microscopic). Most modelling so far limited to 1D with artificial mixing and can only partly account for this.
- Illumination bias: We see mainly what is illuminated by the gamma rays (but this problem is worse in remnants, illuminated by X-rays).

Nebular phase analysis - pros and cons

Photospheric phase → Nebular phase → Remnant phase

Pros:

- Probes the core of the exploded star - SN nucleosynthesis can be inferred.
- Line profiles diagnose the 3D structure and link to explosion physics.
- Less line blending than photospheric phase (lower v and T for emitting gas).
- Limited radiative transfer effects → relatively "clean view".

Cons:

- Complex (mostly NLTE) modelling, and associated challenge in getting physical conditions right.
- Complex mixing in the explosion (macroscopic, maybe some microscopic). Most modelling so far limited to 1D with artificial mixing and can only partly account for this.
- Illumination bias: We see mainly what is illuminated by the gamma rays (but this problem is worse in remnants, illuminated by X-rays).
- SNe rapidly dim → limited S/N of observed spectra.

Results examples

1) Explosive nucleosynthesis

2) Hydrostatic nucleosynthesis

3) Hydrodynamics of expansion

1) Explosive nucleosynthesis: Stable nickel production

Jerkstrand+2015

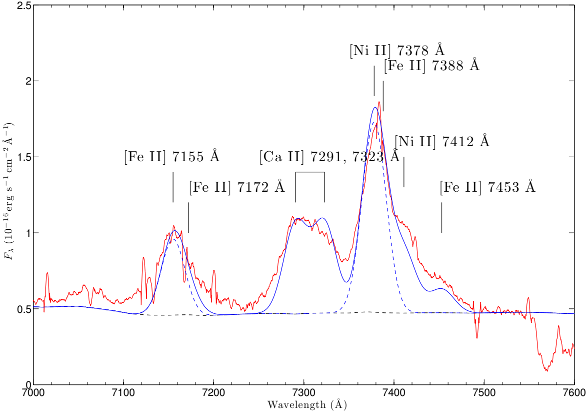

- The **Ni/Fe ratio** ($=^{58-60}$Ni/^{56}Ni at explosion) can be quite **robustly** inferred from [Ni II] 7378 / [Fe II] 7155. Also [Ni II] 1.9 μm useful.

1) Explosive nucleosynthesis: Stable nickel production

Jerkstrand+2015

	SN	Ni/Fe (×solar)	Reference
Solar	1987A	0.5 – 1.5	Wooden+1993, AJ+2015
	2004et	∼1	Jerkstrand+2012
	2012A	∼ 0.5	Jerkstrand+2015
	2012aw	∼ 1.5	Jerkstrand+2015
Super-solar	2006aj	2 – 5	Maeda+2007, Mazzali+2007
	2012ec	2.2 – 4.6	Jerkstrand+2015
Extreme	Crab	60 – 75	Macalpine+1989, 2007

- CCSNe make solar or somewhat supersolar Ni/Fe.
- This constrains Y_e of the layer experiencing explosive oxygen burning (Jerkstrand+2016c).
- We do not see the high $^{58-60}$Ni production expected in ECSNe in any low-velocity SNe (Jerkstrand+2018).

2)Hydrostatic nucleosynthesis : Oxygen

Jerkstrand+2012,2014,2015

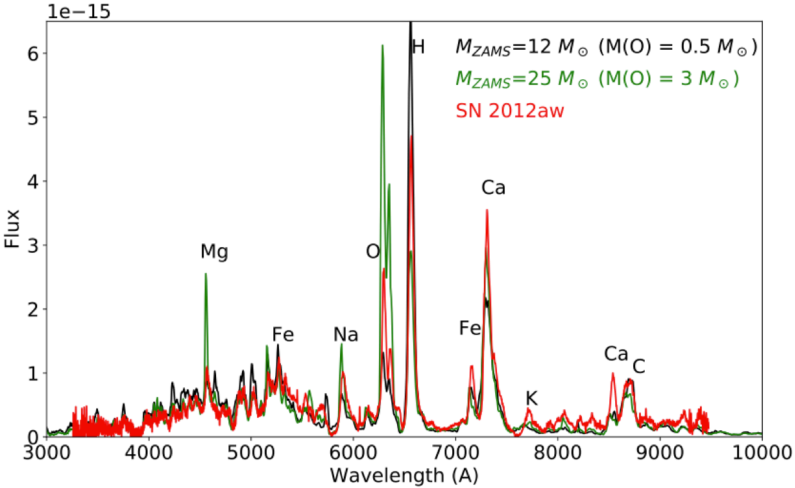

2)Hydrostatic nucleosynthesis : Oxygen

Jerkstrand+2012,2014,2015

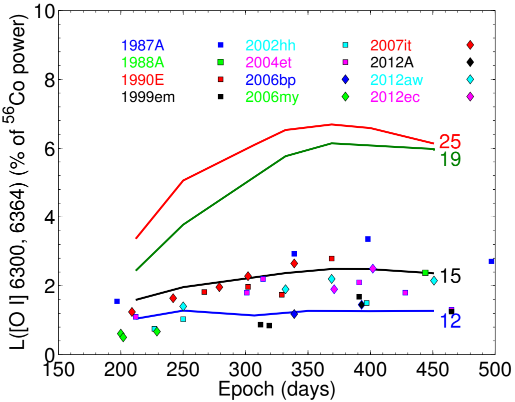

- No sign of stars with He cores $\gtrsim 6-7\ M_{\odot}$ exploding as Type IIP, IIb, or Ib SNe (consistent with latest hydromodelling, Melina's talk).

3)Hydrodynamics

Jerkstrand+2012

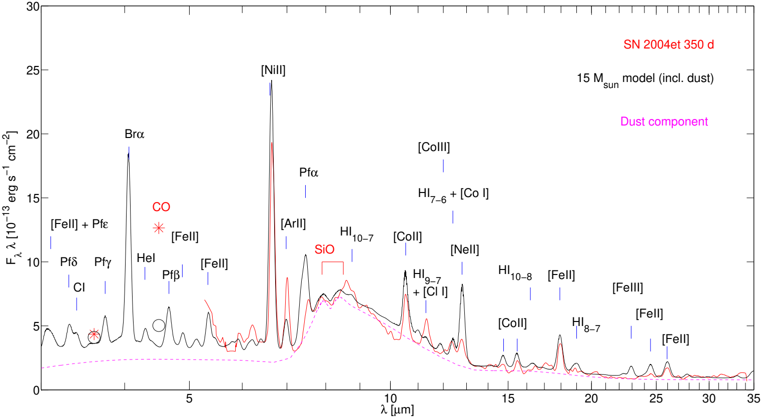

- The MIR lines are optically thick, in LTE, and have $E \ll kT \rightarrow$ (at ∼ 1y) **robust to infer <u>volume</u> of emission**.

3)Hydrodynamics

Jerkstrand+2012

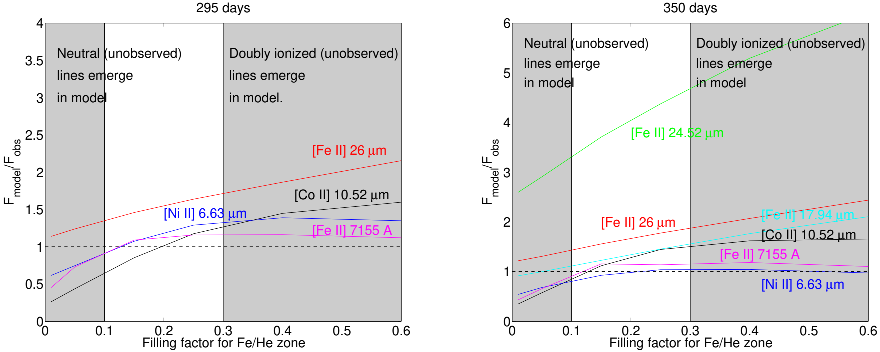

- We can use MIR lines to determine the ^{56}**Ni bubble expansion**. SN 1987A and SN 2004et both give volume filling factor $f \gtrsim 0.2$.

3)Hydrodynamics

Direct comparison to hydromodels (Gabler+2021):

Table 4. Characteristics of the clumps of NiCoFeX after $t \sim 1$ yr for models B15$_0$, B15, B15$_\mathrm{X}$, N20, L15, and W15, respectively. In the different columns, we give the model name, the fraction of mass of the clumps compared to the total mass of NiCoFeX, F_ρ, the threshold density above which we define the clumps, the number of clumps, the number of clumps with NiCoFeX mass larger than $10^{-6}\,\mathrm{M}_\odot$, the volume of the clumps compared to the volumes inside a sphere with the radius where the mean velocities of the material are $\bar{v}_{1500} = 1500$ km s^{-1}, $\bar{v}_{2500} = 2500$ km s^{-1}, and $v^{\mathrm{NiCoFeX}}_{\mathrm{fastest}}$, and finally the surface area in the x–z plane covered by the NiCoFeX clumps compared to a square with side length of twice the radius where the ejecta move with $\bar{v}_{1500}$, $\bar{v}_{2500}$, and $v^{\mathrm{NiCoFeX}}_{\mathrm{fastest}}$, respectively.

Model	F_ρ	$\rho^{\mathrm{min}}_{\mathrm{NiCoFeX}}$ (g cm^{-3})	Number of clumps	Clumps with $M > 10^{-6}\,\mathrm{M}_\odot$	$V^{1500}_{\mathrm{NiCoFeX}}$	$V^{2500}_{\mathrm{NiCoFeX}}$	$V^{\mathrm{fastest}}_{\mathrm{NiCoFeX}}$	$A^{1500}_{\mathrm{NiCoFeX}}$	$A^{2500}_{\mathrm{NiCoFeX}}$	$A^{\mathrm{fastest}}_{\mathrm{NiCoFeX}}$
B15$_0$	0.9	0.021	21	8	0.591	0.127	0.0349	0.799	0.562	0.232
	0.8	0.034	28	11	0.406	0.088	0.0240	0.693	0.483	0.198
	0.7	0.046	41	20	0.288	0.062	0.0170	0.592	0.407	0.166
	0.6	0.057	54	39	0.200	0.043	0.0118	0.514	0.338	0.136
	0.5	0.070	58	36	0.134	0.029	0.0079	0.441	0.264	0.105
	0.4	0.085	60	37	0.085	0.018	0.0050	0.372	0.193	0.075
	0.3	0.105	51	30	0.051	0.011	0.0030	0.294	0.129	0.049
	0.2	0.134	70	34	0.028	0.006	0.0017	0.202	0.081	0.029
	0.1	0.172	129	36	0.012	0.003	0.0007	0.125	0.046	0.017
B15	0.9	0.018	9	6	1.509	0.324	0.0866	0.952	0.721	0.305
	0.8	0.029	13	11	1.210	0.259	0.0694	0.912	0.674	0.283
	0.7	0.041	25	13	0.971	0.208	0.0557	0.864	0.624	0.259
	0.6	0.052	36	23	0.759	0.163	0.0436	0.790	0.565	0.231
	0.5	0.065	50	40	0.565	0.121	0.0324	0.715	0.490	0.199
	0.4	0.079	61	44	0.388	0.083	0.0223	0.643	0.402	0.160
	0.3	0.098	51	32	0.237	0.051	0.0136	0.554	0.300	0.116
	0.2	0.123	53	36	0.121	0.026	0.0070	0.409	0.181	0.066
	0.1	0.163	64	28	0.047	0.010	0.0027	0.268	0.100	0.036

Elements we can diagnose from SN nebular phase spectra

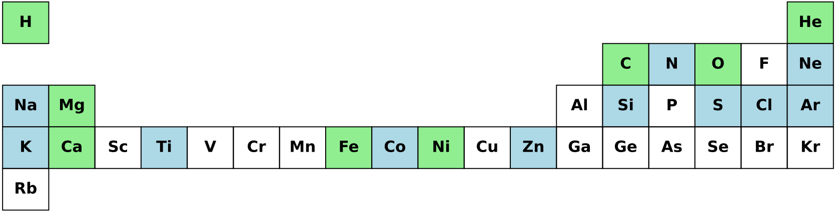

Good diagnostic potential

Moderate diagnostic potential

Challenging to diagnose

3D effects

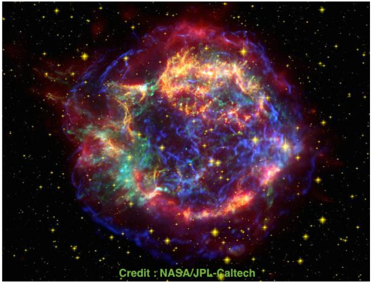

Line luminosities:

- Distribution relative to the ^{56}Ni $\rightarrow$ **illumination**.
- Variation in density $\rightarrow$ **ionization balance**.

Line profiles:

- Test the **bulk velocities** and **degree of asymmetry**.
- Fine-structure $\rightarrow$ **clumping diagnostic**.

* periodic plot: markera in olika förbränningsprocesser
* 87A : starta med quasi-bol LC
* ref ono arbete etc.
* nämn sofies arbete..ta med mol och stoft i "40 yrs of progress".
* förklara utmaningar med 3D modellerningen
* tiden

How SUMO consider multi-D effects (until now)

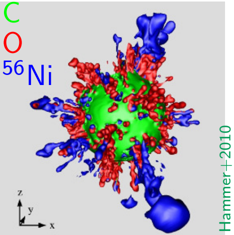

Hammer+2010

Representation in SUMO : **virtual blobs** of different composition. (Jerkstrand+2011)

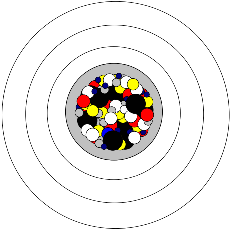

Let blob type $\mathbf{i}$ be characterised by number of blobs $\mathbf{N_i}$ and filling factor $\mathbf{f_i}$. The blob radius is then found from $\mathbf{V_{exp} f_i = N_i \frac{4\pi}{3} R_i^3}$ ($\mathbf{V_{exp}}$ known from line widths). Upon exiting one blob, probability of entering type $\mathbf{i}$ is proportional to its surface area, or

$$\mathbf{p_i = \frac{N_i R_i^2}{\sum N R^2}}$$

3D hydrosimulations to late times

- Neutrino-driven 3D models evolved to late (=homologous) times have been produced by the Garching group Wongwathanarat+2013,2015,2017, Gabler+2021 MNRAS, Stockinger+2020, ApJ

- Opportunity to put explosion models to the test
  - Fastest ^{56}Ni?
  - Bulk velocity of ^{56}Ni?
  - Degree of asymmetry?
  - Composition of Si-burn ashes?

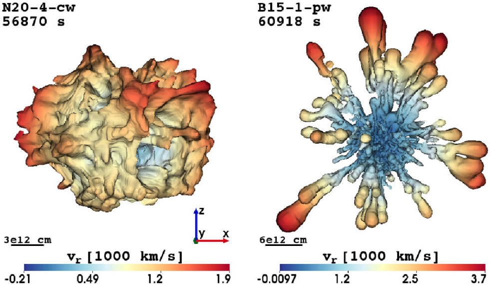

Wongwatharanat+2015

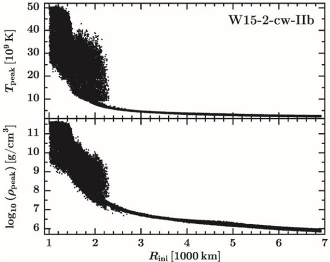

Wongwatharanat+2017

3D modelling: radiative transfer method Jerkstrand+2020

- **Monte Carlo transport in spherical coordinate system**
  - Avoid remapping.
  - Avoid expensive small-cell transport in outer regions, while resolving the small-scale structure in the metal core.
  - More expensive geometry calculations to zone boundaries. Tests show factor few penalty but can be offset by more efficient gridding.

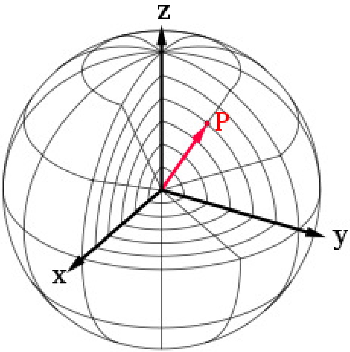

3D hydrodynamic model set explored

$M_{ZAMS} = 15 - 20\ M_\odot$ progenitors exploded with ~1.5 Bethe.

Model	Prog.	E (10^{51} erg)	M_{ejecta} ($M_\odot$)	^{56}Ni bulk speed (km/s)	^{56}Ni asymmetry (km/s)
B15	BSG	1.4	14	1130	145
L15	RSG	1.7	14	1160	398
M15	RSG	1.4	19	1490	473
W15	RSG	1.5	14	1170	517

Wongwatharanat+2015, 2017, Gabler+2021

↑

$\sum_{cells} |v| \Delta m_{56Ni} / M_{56Ni}$

Imprint on **line widths**

↑

$= \mathbf{p_{56Ni}} / M_{56Ni}$

Imprint on **line asymmetries**

Example gamma lines (model L15)

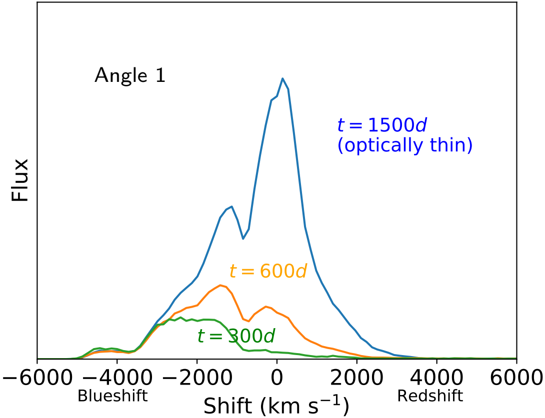

- Lines can have multiple peaks and are generally not “Gaussian”.
- Compton scattering eats away preferentially the red side of the line for several years.

Example gamma lines (model L15)

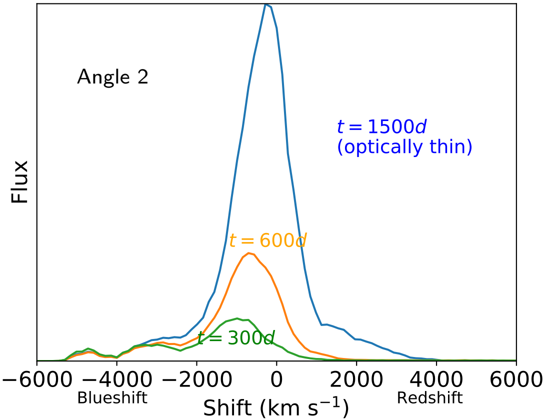

- Lines can have multiple peaks and are generally not "Gaussian".
- Compton scattering eats away preferentially the red side of the line for several years.

Example gamma lines (model L15)

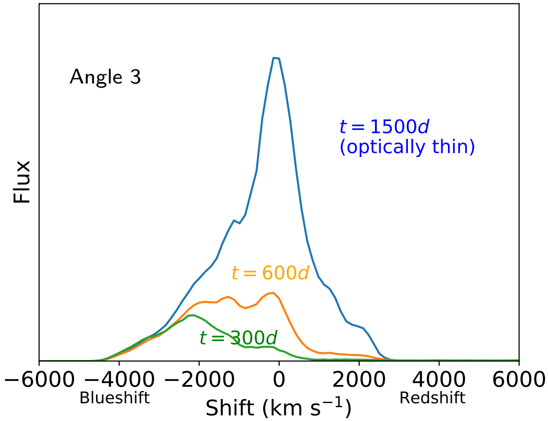

- Lines can have multiple peaks and are generally not "Gaussian".
- Compton scattering eats away preferentially the red side of the line for several years.

SN 1987A : ^{56}Co decay lines show redshifts from ∼400d

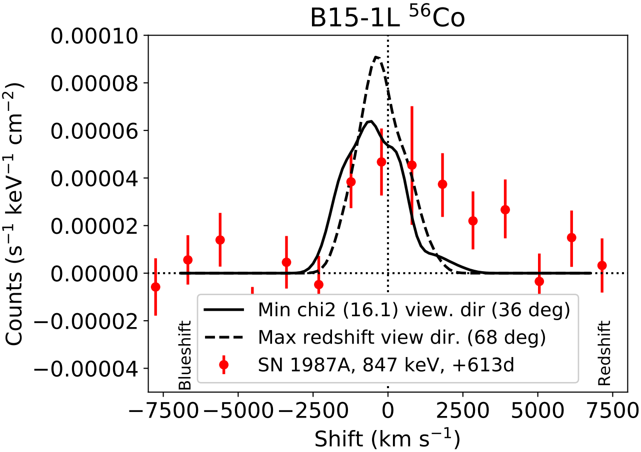

- Models struggle to reproduce emission from receding ejecta with radial velocities up to ∼ 5000 km s^{-1} observed (models reach max ∼3000 km s^{-1}).

SN 1987A : ^{56}Co decay lines show redshifts from ∼400d

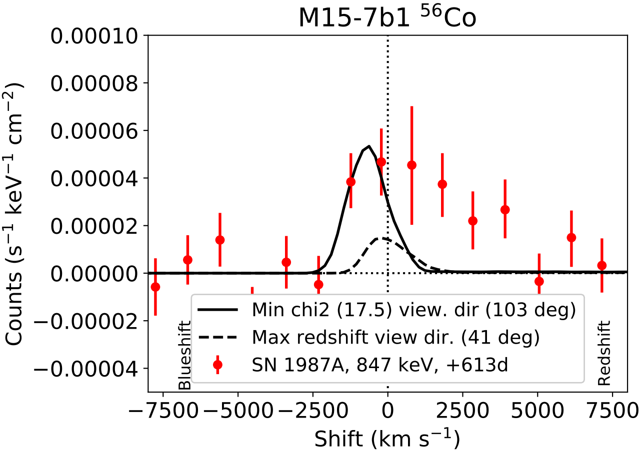

- Models struggle to reproduce emission from receding ejecta with radial velocities up to $\sim$ 5000 km s^{-1} observed (models reach max ∼3000 km s^{-1}).

SN 1987A : ^{56}Co decay lines show redshifts from ∼400d

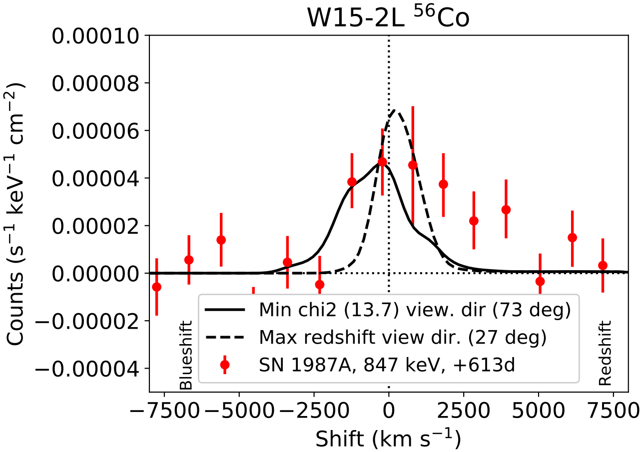

- Models struggle to reproduce emission from receding ejecta with radial velocities up to $\sim$ 5000 km s^{-1} observed (models reach max ∼3000 km s^{-1}).

SN 1987A : ^{56}Co decay lines show redshifts from ∼400d

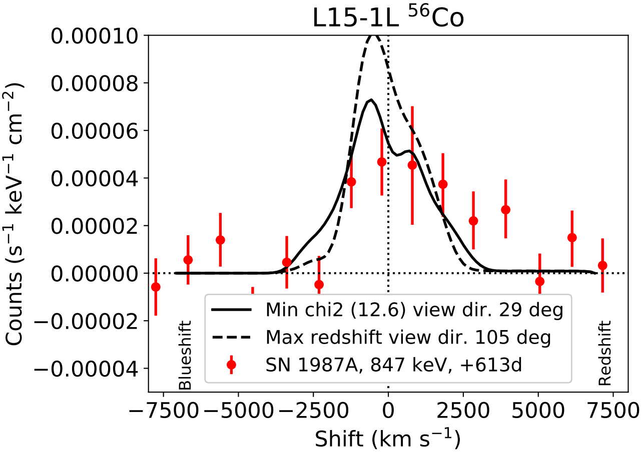

- Models struggle to reproduce emission from receding ejecta with radial velocities up to ∼ 5000 km s^{-1} observed (models reach max ∼3000 km s^{-1}).

Viewing angle variations

Define **shift** and **width** of line:

$$V_{shift} = \frac{\int C_E V(E) dE}{\int C_E dE}$$

$$V_{width} = \frac{\int (V(E) - V_{shift})^2 C_E dE}{\int C_E dE}$$

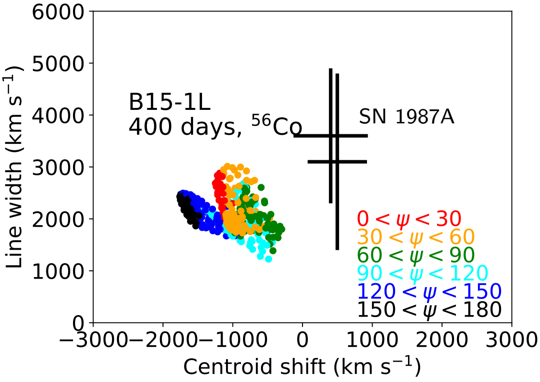

- Shift and width can vary with several 1000 km/s depending on viewing angle.

Viewing angle variations

Define **shift** and **width** of line:

$$V_{shift} = \frac{\int C_E V(E) dE}{\int C_E dE}$$

$$V_{width} = \frac{\int (V(E) - V_{shift})^2 C_E dE}{\int C_E dE}$$

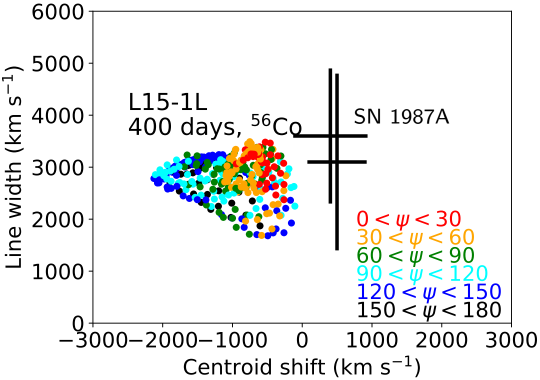

- Shift and width can vary with several 1000 km/s depending on viewing angle.

Infrared iron lines in SN 1987

- Observed NIR lines of Fe/Co/Ni also show redshifts.
- Compared to decay line analysis: better data and optically thin, but more uncertainty for the emissivity (here : $j = d_\gamma \times x_{Fe}$).
- Only one model (L15) gives enough width and asymmetry of the IR lines.

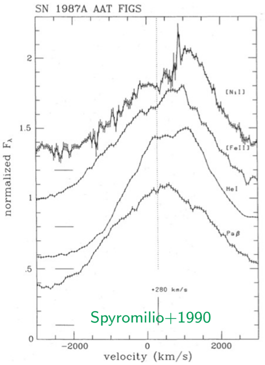

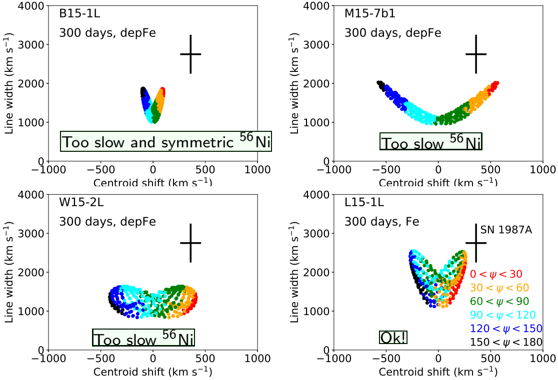

Summary, comparison of current 3D models to SN 1987A

SN 1987A is more extreme in its observed properties of the ^{56}Ni asymmetry and bulk speed than any of the current models.

But - the best models, at the most favorable viewing angles (NS approaching us) are not too far off maybe $\sim 25\%$ too slow ^{56}Ni.

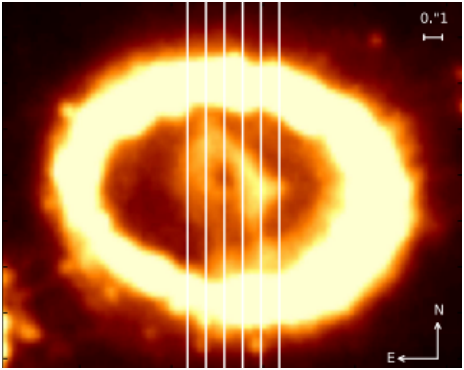

Larsson+2016

Towards 3D models for optical and IR spectra

Next steps:

- Solve for NLTE gas state in each cell. (van Baal, step 1)
- Couple in radiation field. (van Baal, step 2)
- The chemistry. (Cherchneff, Sarangi, Liljegren groundworks)

Discussion points:

- Nebular spectra are sensitive to microscopic composition and clumpiness : to what extent are current Eulerian hydromodels predicting these properties?
- Neutrino-driven models seem quite close to matching SN 1987A : but not quite. What's missing?
- Can we come up with a way to overview and track how each 3D model compares with observations with respect to different observables?

Chemistry

S. Liljegren et al.: The molecular chemistry of Type Ibc supernovae

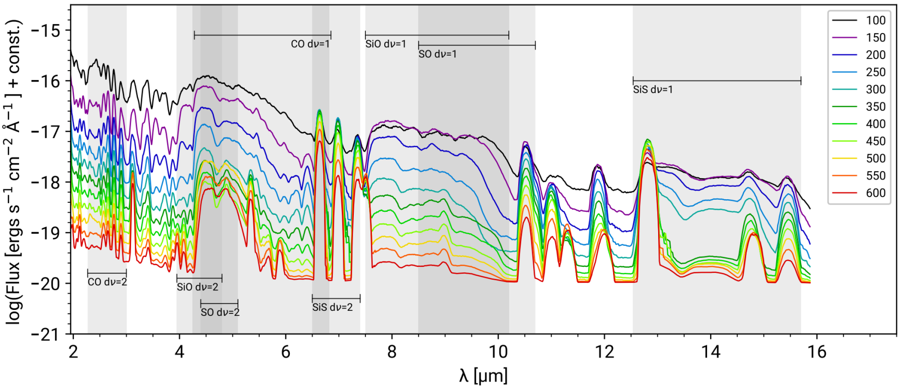

Fig. 8. Model spectra in the MIR, where each line is the spectra at different times in days indicated by the right label, for the standard model. The fundamental (dν = 1) and first overtone (dν = 2) molecular bands are indicated. Unblended molecular emission has a light gray background, blends from two bands mid-gray, and blends from three bands dark gray. The flux here is on a log-scale.